Mecánica Computacional Vol. XXII
M. B. Rosales, V. H. Cortínez y D. V. Bambill (Editores)
Bahía Blanca, Argentina, Noviembre 2003.

HIGH RESOLUTION SCHEMES IN CURVILINEAR GRIDS FOR REDUCING THE GRID ORIENTATION EFFECTS

Clovis R. Maliska and Alexandre O. Czesnat

Computational Fluid Dynamics Laboratory
Mechanical Engineering Department
Federal University of Santa Catarina
88040-900 – Florianópolis - SC
e-mail:maliska@sinmec.ufsc.br, web page: http://www.sinmec.ufsc.br/

Key words: Grid Orientation Effects, Boundary-Fitted Coordinates, Petroleum Reservoir, TVD Schemes

Abstract. *One of the most important tasks in the numerical simulation of fluid flow problems is the reduction of numerical diffusion contained in the solution. Numerical diffusion is caused by the use of first order interpolation schemes in the approximation of the convective terms in the momentum equations. In petroleum reservoir simulation, a similar problem arises when the mobility is interpolated at the interfaces of the control volumes for the mass fluxes calculation. Depending on the interpolation function used for the mobility, the solution may be contaminated with the so-called grid orientation effect, a similar error as the well-known numerical diffusion. The grid orientation effect in petroleum reservoir simulation causes different breakthroughs, even when the production wells are symmetrically located with respect to the injection well in a homogeneous media. Usually, the upwind scheme is employed, due to its ability of promoting numerical stability. The price one pays is the introduction of considerable amount of grid orientation effects. In curvilinear grids the problem is even more general, since the grid can be oriented according to the flow lines. In this work it is presented a numerical scheme, using the black-oil model, for the solution of the classical 3-wells and 5-spot problems with the main goal of analyzing the grid orientation effects. A more general interpretation for the grid orientation effect is also given. The UDS and some TVD schemes used for reducing this error are employed and compared.*

1 INTRODUCTION

The governing equations for the multiphase flow in porous media are the mass conservation for each component and the Darcys's equations relating velocities with the phase potential. They are hyperbolic in nature and the challenging task of numerically solving these equations is the approximation of the convective terms. The *Upstream Differencing Scheme* (UDS) is the widely used scheme in petroleum reservoir simulation due to its simplicity and robustness of the resulting algorithm. However, the amount of numerical diffusion introduced in the solution may be prohibitive. Therefore, new algorithms should be sought for approximating the convective terms in the governing equations. This paper addresses this issue solving the 3-wells-problem using the UDS scheme and three types of TVD schemes aiming the reductions of the grid orientation effects. The governing equations use the mass fraction of each component as dependent variables. This avoids the numerical difficulty caused by the disappearance of the gas phase, situation which happens when the gas totally dissolves in the oil and the formulation uses the saturation as dependent variables.

1.1 The Grid Orientation Effect

The grid orientation effect was primarily reported by Todd *et al*[1]. They use, for demonstrating the effect, the well-known five-spot problem depicted in Figure. 1(a), and the corresponding Cartesian grids employed in Fig. 1(b).

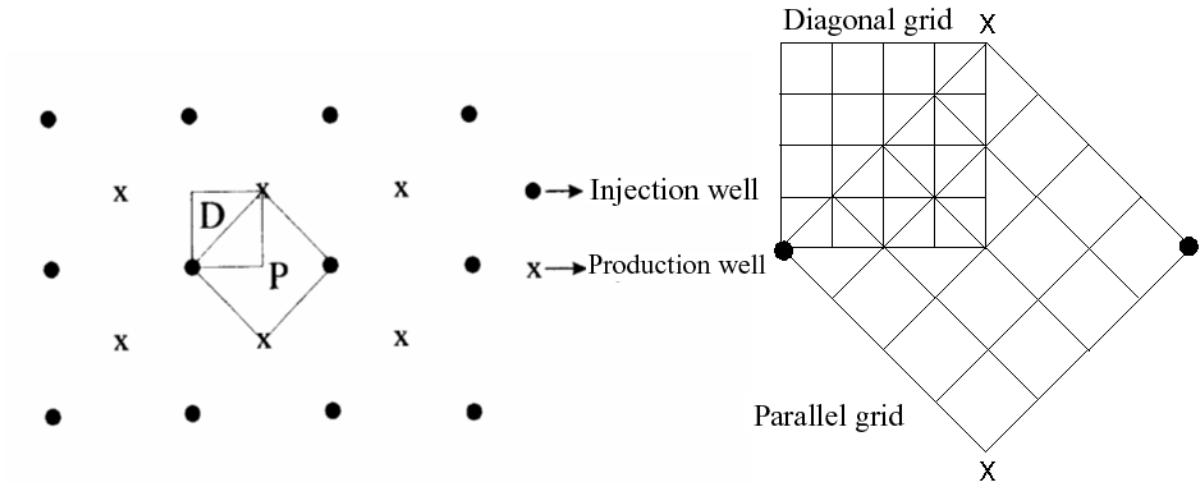

Figure 1: Five Spot Problem Configuration (a) and Cartesian Grids (b)

It can be seen in Figure 1(b) that, depending on the grid used, the line that joins the injection well and the production well is parallel (P) to the coordinate lines or diagonal (D) to the coordinate lines. When using only the five neighboring points, the spatial arrangement related to the flow direction influences the calculation of the mobility at the control volume interfaces

which, in its turn, influences the mass flow calculation. For example, if an *Upstream Differencing Scheme* is used in the parallel grid, both grid points used for the interpolation are aligned with the flow, while in the case of the diagonal grid they are inclined to the flow. This results in a numerical error which retards or speeds up the flow, causing different breakthrough at the producing well depending on the grid.

A definitive explanation of the genesis of the grid orientation effect and its remedy is not yet clear in the literature related to petroleum reservoir simulation. Based on numerical analysis, any approximation of a partial differential equation must recover the exact solution if the approximation is consistent. Consistency requires that the truncation error vanish when refining the grid. Therefore, it would be expected that all differences between the numerical and the exact solution must vanish when the grid is refined. However, Brand *et al*[2], reports that the grid orientation effects does not vanish with the grid refinement when large mobility rates are considered. They state that the solution is always contaminated with numerical diffusion and grid orientation effects. The former vanishes with the grid refinement, improving the sharpness of the front, while the latter keeps distorts the solution according to the grid directions, as the grid gets smaller. They interpret the effects of the grid orientation as a numerical manifestation of a physical instability which arises for high mobility rates.

Yanosik and McCraken[3], using a nine-point scheme for the five-spot problem, reported practically the same results for diagonal and parallel grids using several viscosity ratios, which indicates that interpolation functions involving more grid points may be efficient for reducing the grid orientation effect. Maliska *et al*[4] obtained almost the same results of Yanosik and McCraken[3] using curvilinear coordinates aligned with the flow. Since in real problems it is difficult to always align the grid with the flow, the difficulty with the grid orientation effect persists. Trying to reduce the grid orientation effects, a reasonable large body of literature exists where different interpolation schemes are developed. Among them, the TVD schemes, according to Harten et al[5], is a class of methods which improves the solution quality, without introducing the undesirable numerical oscillations of the higher order schemes. In this direction Rubin and Blunt[6] introduced TVD schemes in the fluxes for the black-oil model em Cartesian coordinates for implicit and explicit formulations. Pinto[7], using non-uniform Cartesian grids employed TVD schemes applied directly on the relative permeability. It was demonstrated that there is almost no differences of applying the TVD schemes in the permeability or in the mass flux. Mota e Maliska[8], extended the Rubin and Blunt schemes to deal with curvilinear coordinates, applying the interpolation in the relative permeability.

In this paper the 3-well problem is solved using TVD schemes in the relative permeability, in a continuation of the work presented by Mota and Maliska[8]. The UDS scheme is also used for comparison purposes.

2 MATHEMATICAL FORMULATION

2.1 Governing Equations

Although the test problems presented in this paper are 2D and for oil-water flow, for

completeness the full model considering oil, water and gas and three dimensions will be presented. The standard black-oil model considers the isothermal flow with immiscible water and oil phases, the water vapor does not take part of the gas phase and the gas is allowed to dissolve in the oil phase.

The mass balances for the three components gives

$$\frac{\partial}{\partial t}\left[\phi\rho^m Z^w\right] = \nabla.\left[\lambda^w \nabla\Phi^w\right] - m^w \tag{1}$$

$$\frac{\partial}{\partial t}\left[\phi\rho^m Z^o\right] = \nabla.\left[X^{oo}\lambda^o \nabla\Phi^o\right] - X^{oo} m^o \tag{2}$$

$$\frac{\partial}{\partial t}\left[\phi\rho^m\right] = \nabla.\left[\lambda^w \nabla\Phi^w + \lambda^o \nabla\Phi^o + \lambda^g \nabla\Phi^g\right] - m^w - m^o - m^g \tag{3}$$

$$Z^g = 1 - Z^w - Z^o \tag{4}$$

where ϕ is the porosity, Φ^p the phase potentials, ρ^m the density of the mixture, λ^p the mobility of phase p, m^w, m^o, and m^g are the water, oil and gas mass flow, respectively, z^i the mass fraction of the i component and, finally, x^{oo} is the ratio of the mass of the oil component in the oil phase by the total mass of the oil phase. Recall that this model allows the gas component to be in the oil phase. The phase potentials are given by

$$\Phi^w = P^o - P^{cow} + \gamma^w z \tag{5}$$

$$\Phi^o = P^o + \gamma^o z \tag{6}$$

$$\Phi^g = P^o + P^{cog} + \gamma^g z \tag{7}$$

where

$$P^o - P^{cow} = P^w \tag{8}$$

$$P^o + P^{cog} = P^g \tag{9}$$

Eq. (3), the global mass conservation, is also known as the pressure equation, since in the iterative procedure it is used to advance this variable. Eqs. (1) and (2) give the mass fractions of the water and oil components, and Eq. (4) the mass fraction of the gas component, explicitly found after the calculation of Z^w and Z^o.Introducing Eqs. (5)-(7) in Eqs. (1)-(3), the governing system of equation can be solved for P^o, Z^o and Z^w. The mobility appearing in the equation system is calculated by

$$\lambda^p = \frac{k k^{rp} \rho^p}{\mu^p} \tag{10}$$

where k, k^{rp} and μ^p are the absolute permeability, relative permeability of the component in the p phase and the viscosity of the phase p.

2.2 Coordinate Transformation and Approximate Equations

It is very common in the real practice of petroleum reservoir simulation the use of only Cartesian grids. Recently great interest in using general grids in engineering tools has emerged in the literature, as in Palagi[9], Heinemann[10], Marcondes and Maliska[11], among others. The methodology presented in this paper uses boundary-fitted grids with the concept of solving the governing equations in the curvilinear coordinate system, with tra transformation shown in Figure 2.

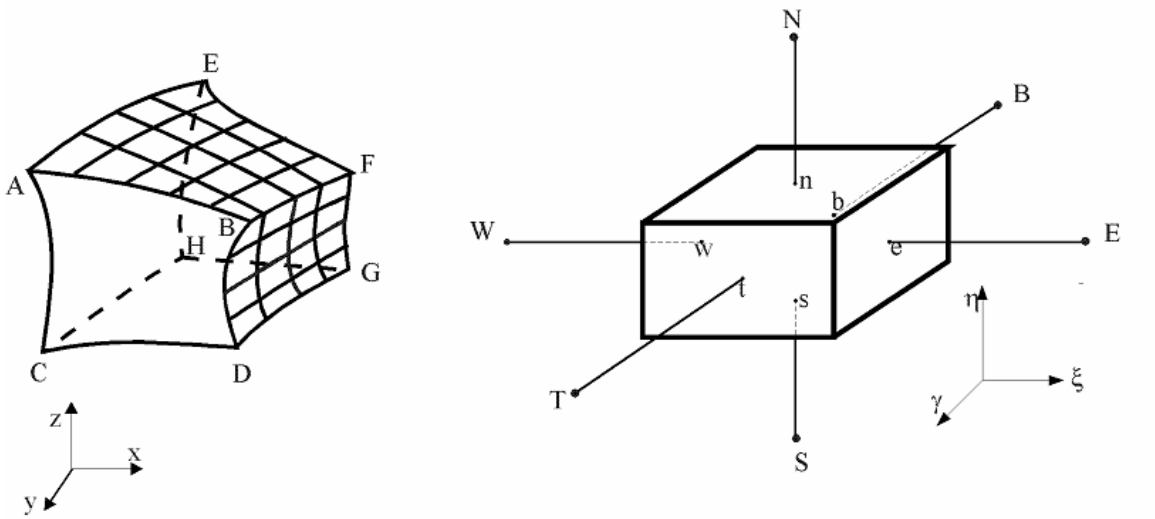

Figure 2: Physical and computational domains

Therefore, the governing equations need to be written in the curvilinear coordinate system. Taking the equation for the water component as example, one has,

$$\frac{1}{J}\frac{\partial}{\partial t}\left(\phi\rho^m Z^w\right)+\frac{m^w}{J}=\frac{\partial}{\partial\xi}\left[D^w_{11}\frac{\partial\Phi^w}{\partial\xi}+D^w_{12}\frac{\partial\Phi^w}{\partial\eta}+D^w_{13}\frac{\partial\Phi^w}{\partial\gamma}\right]+\frac{\partial}{\partial\eta}\left[D^w_{21}\frac{\partial\Phi^w}{\partial\xi}+D^w_{22}\frac{\partial\Phi^w}{\partial\eta}+D^w_{23}\frac{\partial\Phi^w}{\partial\gamma}\right]+$$
$$\frac{\partial}{\partial\gamma}\left[D^w_{31}\frac{\partial\Phi^w}{\partial\xi}+D^w_{32}\frac{\partial\Phi^w}{\partial\eta}+D^w_{33}\frac{\partial\Phi^w}{\partial\gamma}\right] \qquad (11)$$

where J is the Jacobian of the transformation and D^p_{ij} is a diffusion-like coefficient involving physical and geometrical parameters, given by

$$D_{ij}^{p} = \frac{\lambda^{p}}{J}\left[\frac{\partial x^{i}}{\partial x}\frac{\partial x^{j}}{\partial x} + \frac{\partial x^{i}}{\partial y}\frac{\partial x^{j}}{\partial y} + \frac{\partial x^{i}}{\partial z}\frac{\partial x^{j}}{\partial z}\right] \tag{12}$$

with $i, j = 1,2$ or 3, and x^{1}, x^{2}, x^{3} are, ξ, η, γ, respectively.

The transformed equations for the oil component and for pressure (global mass conservation) are similar and will not be reported here. Integration of Eq. (11) in time and over the control volume depicted in Figure 2, considering only the term in the ξ direction to explain the numerical procedure, results

$$\int_{\tau}^{\tau+\Delta\tau}\int_{b}^{t}\int_{s}^{n}\int_{w}^{e}\frac{\partial}{\partial\xi}\left[D_{11}^{w}\frac{\partial \Phi^{w}}{\partial\xi} + D_{12}^{w}\frac{\partial \Phi^{w}}{\partial\eta} + D_{13}^{w}\frac{\partial \Phi^{w}}{\partial\gamma}\right]d\xi d\eta d\gamma d\tau =$$
$$\left[D_{11}^{w}\frac{\partial \Phi^{w}}{\partial\xi} + D_{12}^{w}\frac{\partial \Phi^{w}}{\partial\eta} + D_{13}^{w}\frac{\partial \Phi^{w}}{\partial\gamma}\right]_{e}\Delta\eta\Delta\gamma\Delta\tau - \left[D_{11}^{w}\frac{\partial \Phi^{w}}{\partial\xi} + D_{12}^{w}\frac{\partial \Phi^{w}}{\partial\eta} + D_{13}^{w}\frac{\partial \Phi^{w}}{\partial\gamma}\right]_{w}\Delta\eta\Delta\gamma\Delta\tau \tag{13}$$

Inspecting Eq. (13) one realizes that it is required the evaluation of $D_{ij}^{w}\frac{\partial \Phi^{w}}{\partial x^{i}}$ in the west and east faces of the elemental control volume. These three terms are, in fact, the components of the water flux, which involves the evaluation of the mobility and the derivatives of Φ^{w} at the interfaces. The determination of these fluxes at the interfaces, as a function of the parameters at the grid nodes, requires an interpolation function. This is the key question. If the interpolation function could be exact there would be no generation of truncation errors, as discussed in Maliska[12], and no numerical diffusion or grid orientation effects could be present in the solution. Since it is impossible to obtain the exact interpolation function (to do this it would require the exact solution), the numerical solution is always contaminated with truncation errors. These truncation errors, when associated to certain terms of the partial differential equation receive different nominations, like numerical diffusion and grid orientation effects.

It can be shown that the terms in the brackets of the right hand side of Eq. (13) can be written as

$$\lambda^{p}\frac{\partial \Phi^{w}}{\partial \vec{n}} = (G_{11}\Phi_{\xi}^{w} + G_{12}\Phi_{\eta}^{w} + G_{13}\Phi_{\gamma}^{w}) \tag{14}$$

$$G_{ij} = \frac{D_{ij}^{p}}{\lambda^{p}} \tag{15}$$

what means that the evaluation of the terms in the brackets amounts in calculating $\lambda^{p}\frac{\partial \Phi^{w}}{\partial \vec{n}}\Big)_{e}$

and $\lambda^p \frac{\partial \Phi^w}{\partial \vec{n}}\Big)_w$. What it is usually done is to evaluate the gradient of the phase potential in the best way possible trying not to make the computational stencil too complex, and apply other interpolation function in the mobility. In this work the normal derivative is calculated using a 9-point stencil and the mobility using TVD schemes and the UDS for comparisons.

The system of equations is solved using the Newton's method. The Taylor series expansion of the residue gives

$$\left(F_P^i\right)^{k+1} = \left(F_P^i\right)^k + \sum_{\forall X}\left(\frac{\partial F_P^i}{\partial X}\right)^k \Delta X = 0 \tag{16}$$

where $i = P, w, o$, and $X = Z^w, Z^o, P$, evaluated at the control volume P and its 6 direct neighboring control volumes. Expanding this equation for the water component one gets

$$\left(\frac{\partial F_P^w}{\partial P^{wf}}\right)\Delta P^{wf} + \left(\frac{\partial F_P^w}{\partial P_P}\right)\Delta P_P + \left(\frac{\partial F_P^w}{\partial Z_P^w}\right)\Delta Z_P^w + \left(\frac{\partial F_P^w}{\partial Z_P^o}\right)\Delta Z_P^o + \sum_{NB}\left[\left(\frac{\partial F_P^w}{\partial P_{NB}}\right)\Delta P_{NB} + \left(\frac{\partial F_P^w}{\partial Z_{NB}^w}\right)\Delta Z_{NB}^w + \left(\frac{\partial F_P^w}{\partial Z_{NB}^o}\right)\Delta Z_{NB}^o\right] = -F_P^w \tag{17}$$

All cross-derivatives of the type $\frac{\partial \Phi}{\partial \xi}\Big)_n$ is treated explicitly, therefore the Jacobian matrix will contain seven block diagonals, instead of 19 block diagonals if all cross-derivatives were treated implicitly. This strategy may affect the convergence of the method, depending on the importance of the cross-terms, which are dependent on the non-orthogonality of the grid. All cross-derivative terms are zero if the mesh is orthogonal. The resulting coupled linear system of equation is solved using incomplete LU decomposition.

2.3 Interpolation Schemes

The first scheme to be used is the UDS, which allow identifying the truncation errors caused by this interpolation. In this scheme if

$$\lambda^p \frac{\partial \Phi^w}{\partial \vec{n}}\Big)_e < 0 \tag{18}$$

the mobility at the interface is given by

$$\lambda_e^w = \lambda_P^w \tag{19}$$

The results using UDS will be compared with some TVD schemes. TVD schemes introduce an anti-diffusive term to the UDS and a limiter which enforces, in regions of small gradients, a second order accuracy, and in regions of sharp gradients a first order approximation. As already state, in this work the TVD schemes are applied to the mobility. The mobility, taking the east face as example, can be calculated by

$$\lambda_e = \lambda_e^{UDS} + \left[A_e \Psi\left(r_e^{UDS}\right)\right]^* \tag{20}$$

where A_e, Ψ, r_e^{UDS} and λ_e^{UDS} are the second order term, the flux limiter, the ratio of successive second order terms and the mobility immediately upstream to the face in consideration. The second order term and its ratio are given by

$$A_e = \frac{\vec{L}_{UDS}^{\xi}}{2} \bullet \vec{\nabla}\lambda_e \tag{21}$$

$$r_e^{UDS} = \frac{A_{e-upstream}}{A_e} \tag{22}$$

where

$$\vec{L}_{UDS}^{\xi} = \left(\Delta\xi \cdot x_\xi \hat{i} + \Delta\eta \cdot y_\xi \hat{j} + \Delta\gamma \cdot z_\xi \hat{k}\right)_{UDS} \tag{23}$$

is the length vector em the ξ direction related to the volume immediately upstream the east face, and $\vec{\nabla}\lambda_e$ is the mobility gradient at the east face. The application of this scheme is now exercised. If

$$\left.\frac{\partial \Phi}{\partial \vec{n}}\right)_e < 0$$

then

$$\lambda_e = \lambda_P + A_e \Psi(r_P) \tag{24}$$

$$A_e = \frac{\vec{L}_P^{\xi}}{2} \bullet \vec{\nabla}\lambda_e \tag{25}$$

$$A_w = \frac{\vec{L}_P^{\xi}}{2} \bullet \vec{\nabla}\lambda_w \tag{26}$$

$$r_P = \frac{A_w}{A_e} \tag{27}$$

For a Cartesian grid, for $\Psi(r) = 1$ one obtains a second order scheme, $\Psi(r) = r$ a two-points upstream scheme, $\Psi(r) = 0$ a one-point upstream and for $\Psi(r) = 2$ a one point forward scheme. The flux limiter for a TVD with a Van Leer limiter is calculated by

$$\Psi(r) = \frac{|r| + r}{1 + |r|} \tag{28}$$

in the Sweby region given by $0 \le \Psi(r) \le min(2, 2r)$. The TVD with a third order limiter is calculated by

$$\Psi(r) = \frac{1}{3}(2 + r) \tag{29}$$

Pinto[7] has shown that the above limiter is known to be out of the Sweby region in some parts of the domain, and it is suggested to restrict the 3rd order limiter in the Sweby region. This is done is this work. Pinto[6] also reports that if this is not done, it may not have the TVD properties.

3 RESULTS AND DISCUSSIONS

As a first test problem the 3-wells configuration will be solved. This problem, devised by Hegre et al[13], is depicted in Figure 3 with the geometrical data given in Table 1. For this analysis, a Cartesian and a curvilinear grid are used, as shown in Figures 4 and 5 for 60° and 80°, respectively. The Cartesian grid is a particular case of the curvilinear grid when the angle is 90°. This angle is measured between the horizontal line joining the production wells and the grid line passing by the injection well.

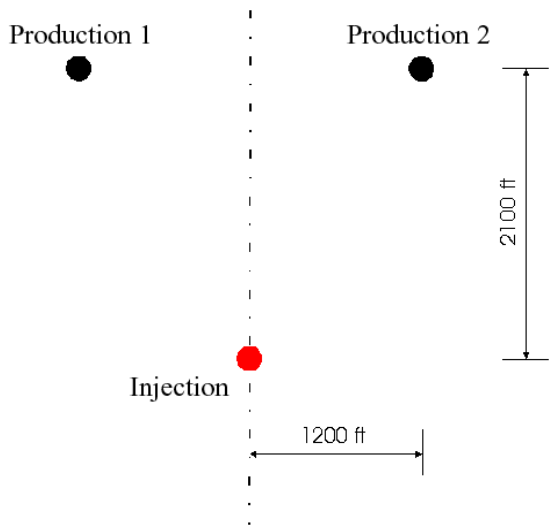

Figure 3: Geometry of the 3-wells problem

Table 1: Three-wells problem data

Porous volume	1.62×10^{7} m^3
Porosity	0.19
Porous volume at the well cells	2.86×10^{4} m^3
Flow rate at injector well	3.53×10^{-3} m^3/s
Flow rate at production wells	1.84×10^{-3} m^3/s

It can be seen in Figure 3 that the injection and production wells are symmetrically located. Therefore, the breakthrough should happen at the same time for both production wells. The problem was solved initially with a Cartesian grid, hence symmetric with respect to the wells, with two grid sizes, 25x22 and 75x66. As expected, the breakthroughs at the two production wells are identical for each grid, since the truncation error propagates symmetrically, as shown in Figure 6. The solutions for two grids are, also as expected, different from each other, due to the grid refinement. The finer grid retards the breakthrough, what follows the right trend, since finer grid reduces the numerical diffusion in the propagating front.

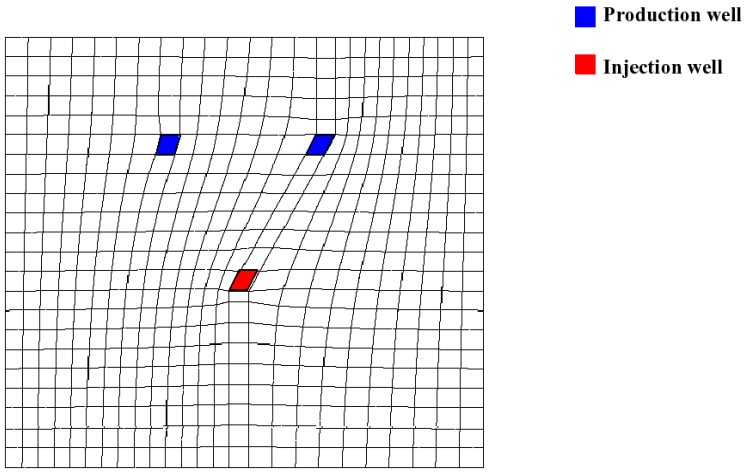

Figure 4: The 3-wells problem with 60^o in the grid

Figure 6 serves, therefore, to identify the truncation errors and to speculate about its nature. The difference in breakthrough times can be viewed as a grid orientation effect, since when the grid has no preferable orientation this difference does not appears. The breakthrough time, however, is wrongly calculated. If the grid is refined, still for the symmetric Cartesian grid, the results improve, reducing the numerical diffusion effect. The grid orientation effect can be viewed, therefore, as a non-homogeneous numerical diffusion, at least for low mobility rates where physical instabilities are not present (Brand *et al*[2]).

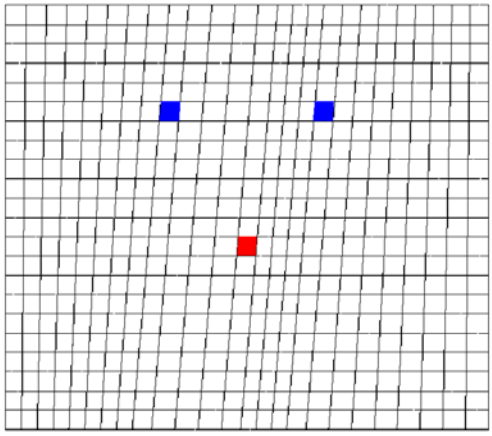

Figure 5: Curvilinear grid for 80°.

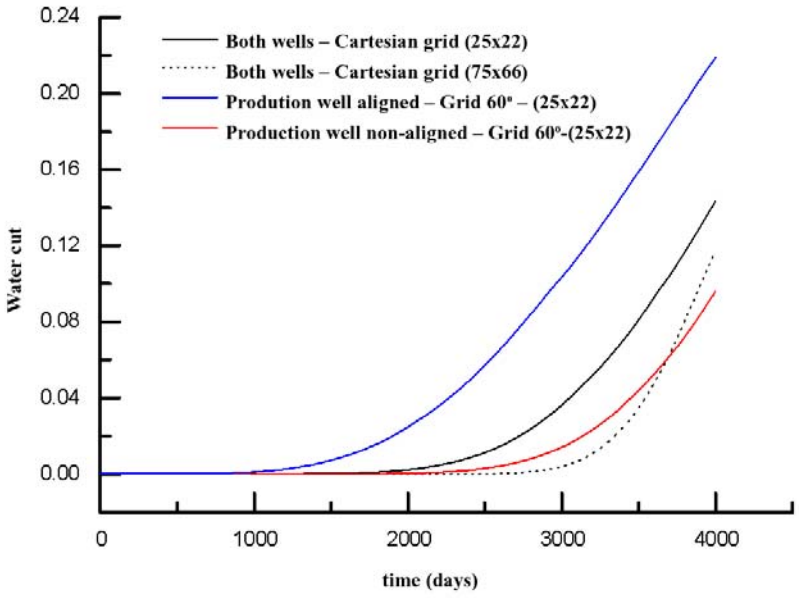

Figure 6: Water cut for the 3-well problem- 60°.

Figure 7 shows the solution for the 3-well problem for the grid with 80°. It can be concluded that the finer Cartesian grid is best result, since it retards the breakthrough, as expected. The results for the curvilinear grid are getting closer to each other, since the curvilinear grid with 80° show small non-symmetry of the grid.

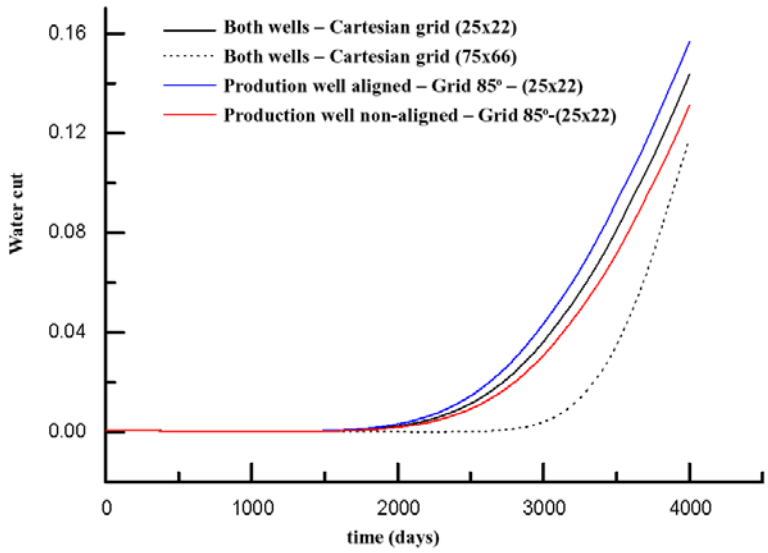

Figure 7: Water cut for the 3-well problem- 80º

The second test problem is the 5-spot configuration shown in Figure 1. The geometrical data is given in Table 2 and the relative permeability in Table 3. The 5-spot configuration consists of 1 well (injector or producer) surrounded by 4 wells (producers or injectors). For the diagonal grid the size of the domain is $(1/4)$ of the 5-spot geometry and $(1/2)$ for the parallel grid. For this reason the grid for the parallel case is 1000mx1000mx5m multiplied by a factor $\sqrt{2}$. Two grid sizes were used: 10x10 and 30x30 for the diagonal grid, and 14x14 and 42x42 for the parallel grid, keeping the factor $\sqrt{2}$ sizing the control volumes.

Table 2–Five-spot problem data	
Initial pressure	3000 psi
Initial water saturation	0.0
Tickness	0.1 m
Lenght	1.0 m
Width	0.1 m
Porosity	0.3
Density	$\rho^w = \rho^o = 1000$ kg/m^3
Viscosity	$\mu^w = \mu^o = 1$ cp
Volume Formation Factor	$B^w = B^o = 1$
Absolut permeability	1.013e3 mD
Water relative permeability	S^w
Oil relative permeability	S^o
Injected flow rate of water	1.25e-2 STB/d
Liquid flow rate produced	1.25e-2 STB/d

Table 3: Data for the 5-spot problem

Oil relative permeability	S^o
Water flow rate injected	9.20×10^{-3} m^3/s
Produced liquid (oil+water)	9.20×10^{-3} m^3/s
Maximum time step (Δt)	10 days (8.64×10^5 s)
Minimum time step (Δt)	10^{-8} days (8.64×10^{-4} s)

Figure 8 compares several cases run for the 5-spot problem using UDS and TVD schemes with the semi-analytical solution of Le-Blanc and Claude[14]. In this figure PVI is the number of porous volume injected and is a dimensionless time step. Knowing the water flow rate and PVI it is possible to determine the physical time. In Figure 8 the comparison is made among the 3rd order TVD against the UDS scheme. It is again observed that the UDS scheme is the poorest one for determining the breakthrough time, persisting the differences along time in the predicted water cut. The 3rd order TVD scheme improves considerably the quality of the results for both grids. It also can be seen that the determination of the breakthrough time and the curve behavior for the water cut matches a lot better the semi-analytical solution.

A detailed comparison among the TVD schemes including the Van Leer and ENO (Essentially non-Oscilatory) can be found in Czesnat[15], where all these schemes were applied for Cartesian and curvilinear grids, with the formulation presented in this paper.

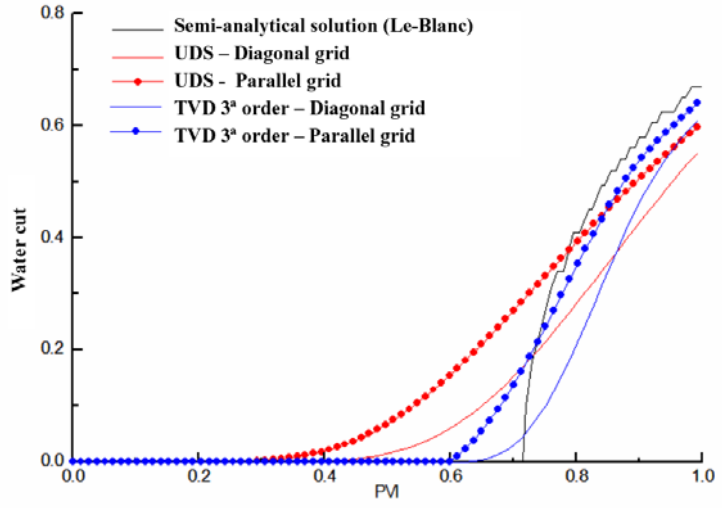

Figure 8: Five-Spot problem. UDSxTVD

4 CONCLUSIONS

This paper advanced a numerical formulation for three-dimensional three-phase flows

encountered in petroleum reservoir simulation. The methodology was applied to solve two-dimensional problems with the main goal of analyzing the grid orientation effects. Two problems were solved, the 3-wells and the well-known 5-spot problem using UDS and TVD schemes. Some of the conclusions presented herein are based on results not shown in this paper. Five points UDS schemes always introduce excessive numerical diffusion anticipating the breakthrough time and smearing the sharp front. TVD schemes, in the other hand, show less numerical diffusion and are free of oscillations. For application in petroleum reservoir simulation they are simple to apply. An important conclusion of the study can be draw: high resolution five-point schemes are able to better predict the sharp fronts, but the influence of the grid orientation remains. This means that these schemes reduce the local numerical diffusion but still keeping it non-homogenous. If high resolution nine-point schemes are applied this non-homogeneity is also reduced. This implies that the grid orientation effects are part of the numerical diffusion, at least for the low mobility problems solved. Therefore, the improvement in the flow calculation requires higher resolution schemes with more grid points involved.

5 REFERENCES

[1] Todd, M. R., O'Dell, P. M., e Hirasaki, G. T., "Methods for Increasing Accuracy in Numerical Reservoir Simulators", SPE J., pp. 515-530, Dez. (1972).

[2] Brand, C. W., Heinemann, J. E., Leoben, M. U. and Aziz, K., "The grid Orientation Effect in Petroleum Reservoir Simulation", SPE Paper 21228, p. 275-286, Anheim, California, (1991).

[3] Yanosik, J. L. e McCracken, T. A., "A Nine-Point, Finite-Difference Reservoir Simulator for Realistic Prediction of Adverse Mobility Ratio Displacements", SPE J., pp. 253-262, Fev. (1976).

[4] Maliska, C.R., Silva, A. F. C., Jucá, P. C. S. and Livramento, A.R., "Desenvolvimento de um Simulador 3D Black-Oil em Coordenadas Curvilíneas Generalizadas, Parte I, Relatório para a Petrobrás/Cenpes, Sinmec/UFSC, (1993).

[5] Harten, A., Engquist, B., Osher, S. e Chakravarthy, S., "Uniformly High-Order Accurate Essentially Non-oscillatory Schemes, III", J. Comput. Phys. 71, 231 (1987).

[6] Rubin, B. Blunt, M. J., "Higher-Order Implicit Flux Limiting Schemes for Black-Oil Simulation" Proceedings of the 11º SPE Conference, California, (1991).

[7] Pinto, A. C. C., "Esquemas de Alta Resolução para Controle de Dispersão Numérica em Simulação de Reservatórios", Dissertação de Mestrado, UNICAMP, São Paulo, Nov. (1991).

[8] Mota, M. A. A., Maliska, C. R., "Simulação Numérica de Reservatórios de Petróleo Utilizando Coordenadas Generalizadas e Interpolação TVD", Anais do V ENCIT, p.325-328, São Paulo, Brasil, (1994).

[9] Palagi, C., "Generation and Application of Voronoi Grids to Model Flow in Hoogeneous Reservoir", Ph. D. Dissertation, Stanford University, USA, (1992).

[10] Heineman, G. F., Heinemann Z. E.,"Gridding Concept for Third Generation Reservoir

Simulators", Sixt International Forum on Reservoir Simulation, Hof/Salzburg, Austria, September, (2001).
[11] Marcondes, F., Zambaldi, M. C., Maliska, C. R., "Comparação de Métodos Estacionários e GMRES em Simulação de Reservatórios de Petróleo Utilizando Malhas Não-estruturadas de Voronoi", J. of the Braz. Society of Mechanical Sciences, vol. XVII, n.4, p. 360-372, (1995).
[12]Maliska, C. R., "Transferência de Calor e Mecânica dos Fluidos Computacional", Ed. LTC - Livros Técnicos e Científicos Editora S. A., Rio de Janeiro, Rj, Brasil (1995).
[13]Hegre, T. M., Dalen, V., Henriquez, A., "Generalized Transmissibilities for Distorted Grids in Reservoir Simulation", Paper SPE 15622, Proc. SPE 61st Annual Technical Conference and Exhibition, pp. 15, New Orleans, (1986).
[14]Le Blanc, J. L.,Claude, B. H.,"A Streamline Model for Secondary Recovery », SPE Journal, 7-12, March, (1971).
[15]Czesnat, A., O, "Implementação de Esquemas de Interpolação para a Minimização da Difusão Numérica em Simulação de Reservatórios de Petróleo", Dissertação de Mestrado, Curso de Pós-Graduação em Engenharia Mecânica, UFSC, Florianópolis, Sc, Brazil, (1999).

6 ACKNOWLEDGEMENTS

The first author gratefully acknowledges the ANP-Agência Nacional de Petróleo, from Brazil, for the partial support of this work.